Electronic and superconducting properties of silicon and carbon clathrates

D. Connétable, X. Blase*

Laboratoire de Physique de la Matière Condensée et Nanostructures, Université Claude Bernard-Lyon 1 and CNRS (UMR 5586), Bât. 203, 43 Bd du 11 Novembre 1918, 69622 Villeurbanne Cédex, France

Abstract

We review the electronic properties of pure and doped silicon and carbon clathrates. Using accurate quasiparticle calculations within the GW approximation, we show that undoped clathrates are ~1.8 eV band gap semiconducting compounds. Further, the effect of doping by elements more electronegative than Si is shown to lead to p-type doped semiconductors with a ~2.3–2.5 eV band gap in the visible energy range. Similar results are observed under doping of hydrogenated Si_n ($n = 20, 24, 28$) clusters and rationalized on the basis of group theory analysis. Finally, the superconducting properties of doped clathrates are discussed. We show that superconductivity is an intrinsic property of the standard silicon sp^3 environment provided that efficient doping can be achieved.

Keywords: Clathrates; Electronic properties; Superconductivity; Ab initio calculations; Quasiparticle study

1. Introduction

Silicon clathrates, first synthesized in 1965 by Kasper et al. [1], are interesting materials: they crystallize in a local sp^3 environment, as in the well-known diamond phase (labeled Si-2 in what follows) but, unlike the dense Si-2 phase, clathrates are low-density materials allowing significant doping. Such systems are therefore unique to study the electronic and superconducting properties of highly doped column IV semiconductors.

Si-clathrates are composed of face sharing Si_{20}, Si_{24} and Si_{28} clusters. Several types of structure exist. In the type-I phase (see Fig. 1), only Si_{20} and Si_{24} cages are present, while in the type-II structure, Si_{20} and Si_{28} cages are building the network. While first synthesis were performed using a chemical route [1], more recent techniques [2][1] are based on the phase transformation under pressure and temperature ($P \sim 3$–5 GPa and $T \sim 800$ °C) of a mixture of Si diamond powder and another element X (X = Na, Ba, K, I, etc.). When pressure is released, X-ray analysis shows well-crystallized micro-grains of e.g. X_8@Si-46 (type-I) clathrates, where the X element is located as a single atom in the center of all cages [3].[2] One thus obtain heavily doped silicon sp^3 networks by endohedral intercalation. In the case of small X = Na doping, heat treatment can be shown to lead to diffusion out of

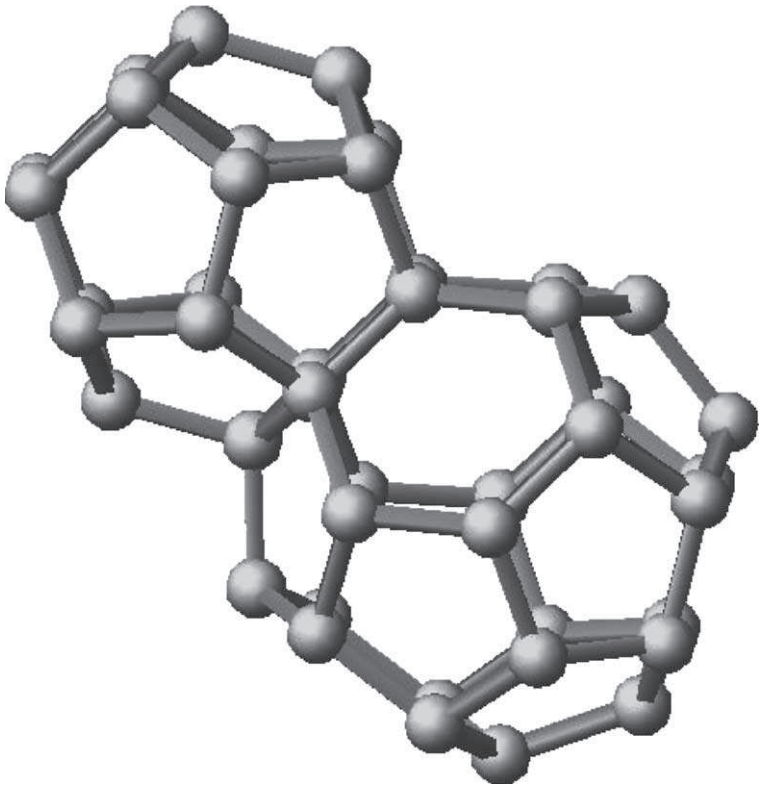

Fig. 1. Symbolic representation of face sharing Si_{20} and Si_{24} cages as building unit of type-I clathrates.

the crystal of most of the intercalated Na atoms, leading to relatively pure Si-46 clathrates.

While empty clathrates have interesting intrinsic properties as shown below, the properties of ''doped'' or intercalated X_8@Si-46 systems are certainly more promising and many novel properties are hinging on doping. For example, it has been shown that iodine [4] or xenon doped silicon clathrates can exhibit a band gap in the visible range [5]. This large value of the band gap, together with the $\sim$8 K superconductivity of Ba-doped clathrates [6], the low compressibility of such phases [7] and their high thermoelectric power [8,9] explain that these compounds have recently generated much interest more than three decades after their first synthesis.

In the present paper, we review the properties of bare and doped clathrates. In a first section, as a reference, we provide an accurate quasiparticle study of the band structure of silicon and carbon clathrates within the so-called GW approximation. In a second part, the effect of doping by elements more electronegative than silicon (p-type doping) is presented and shown to lead potentially to silicon-based materials with a band gap in the visible range. Similar results are observed under doping of hydrogenated Si_n ($n = 20, 24, 28$) clusters and rationalized on the basis of group theory analysis. Finally, we study the superconductivity of Ba-doped clathrates within the standard BCS theory, with electron–phonon coupling matrix elements calculated from perturbative density functional theory (DFPT). The origin of the superconductivity in such systems and the case of carbon clathrates is discussed.

2. Electronic properties of bare silicon and carbon clathrates

The case of bare clathrates, apart from the interest one may find in their specific properties, provides a

necessary reference point to further understand the effect of doping or intercalation. As no photoemission data is available so far, the exact nature of the band structure and band gap of clathrates have been discussed on the basis of tight-binding [10] and ab initio density functional [11] (DFT) calculations [10,12–15]. In particular, DFT studies within the local density approximation [16] (LDA) predicts [10,13,15] that the type-II Si-34 phase is a ''nearly-direct'' band gap material and that this gap is ~0.7 eV larger than the one of bulk Si-2 diamond [17].[3] The possible direct nature of the gap and its large value suggest that Si clathrates are very good candidates for electronic and opto-electronic applications.

DFT-based band structure calculations are however known to lead to large discrepancies as compared to experimental results. The most documented problem is related to the magnitude of the band gap of semiconductors and insulators which is significantly underestimated [18].[4] In this section, we present an accurate first-principles quasiparticle study of the electronic properties of Si-34 clathrates. Our approach is based on the so-called GW approximation [20,21] which has been shown to provide for semiconductor bulk [21] and surfaces [19] quasiparticle energies accurate to within 0.1 eV as compared to photo-emission experiments. Within this approach, we find that Si-34 is a 1.85 eV direct band gap material. Further, the quasiparticle correction at high symmetry points for the doped Xe_8@Si-46 phase is calculated, showing that doped clathrates can exhibit a band gap in the visible range. We finally predict the quasiparticle properties of the hypothetical C-34 and C-46 phases.

2.1. Technical details

The computation of the quasiparticle energy is achieved using a self-energy formalism [20]. In this approach, we keep a one-electron picture by solving, as in the Kohn–Sham formalism, a one-body Schrödinger-like equation, but the LDA exchange-correlation functional is replaced by a ''self-energy'' operator Σ which is non-local, energy-dependent and non-Hermitian in general. In the GW approximation [20,21] used in this calculation, the self-energy Σ is taken to be the first order term in an expansion in successive powers of the screened inter-electronic interaction W, namely:

$$\Sigma(\boldsymbol{r},\boldsymbol{r}';E) = \mathrm{i}\int \frac{\mathrm{d}E'}{2\pi}\mathrm{e}^{-\mathrm{i}\delta E'}G(\boldsymbol{r},\boldsymbol{r}';E-E')W(\boldsymbol{r},\boldsymbol{r}';E'), \tag{1}$$

where G is the dressed one-particle Green's function. Our approach [21] is to make the best possible approximation for G and W. As shown in previous GW calculations for Si- or C-based semiconductors and insulators, the LDA wavefunctions accurately describe the quasiparticle wavefunctions so that we may write:

$$G(E) = \sum_{n\boldsymbol{k}} \frac{|n\boldsymbol{k}\rangle\langle n\boldsymbol{k}|}{E - E^{\mathrm{LDA}}_{n\boldsymbol{k}} - \mathrm{i}\eta}, \tag{2}$$

with $|n\boldsymbol{k}\rangle$ the LDA eigenfunctions and $E^{\mathrm{LDA}}_{n\boldsymbol{k}}$ the LDA energies (η is a negative/positive infinitesimal for energies above/below the Fermi energy).

The screened coulomb potential W is calculated using the dielectric matrix $\epsilon_{\boldsymbol{q}}(\boldsymbol{G},\boldsymbol{G}')$ obtained within the random-phase approximation (RPA) [22] and expressed in reciprocal-space [23] ($\boldsymbol{q}$ samples the Brillouin zone and $(\boldsymbol{G},\boldsymbol{G}')$ are reciprocal lattice vectors). In the evaluation of the dielectric response and self-energy operator, the DFT-LDA spectrum is used as the zeroth order set of eigenvalues and eigenstates in a first-order perturbation-like approach. Up to 850 conduction states have been used in the summation over unoccupied states appearing in the expression of the susceptibility and self-energy operators. A cut-off of 3.0 and 3.5 a.u. for Si and C, respectively was used for the magnitude of the $|\boldsymbol{q}+\boldsymbol{G}|$ basis vectors considered to build the $\epsilon_{\boldsymbol{q}}(\boldsymbol{G},\boldsymbol{G}')$ matrix. More technical details can be found in Ref. [21].

2.2. Quasiparticle band structure of Si-34

As a first step, we study the DFT-LDA band structure of Si-34. We use standard pseudopotential [24,25] and expand the wavefunctions on a planewave basis with a maximum kinetic energy of 16 Ry. The exchange-correlation functional within the LDA is

[3] Another form of large gap cage-like silicon sp^3 system was proposed in [17]. This phase, affiliated to clathrates, was labeled Hex-Si_{40} and will not be studied here.

[4] This can be shown to be related to the discontinuity of the exchange-correlation potential across the band gap which is not accounted for within the DFT (see (e.g.) [18]).

based on the parametrization provided by Perdew and Zunger [26] of the numerical data of Ceperley and Alder [27]. We use two irreducible $\boldsymbol{k}$-points [28] to sample the irreducible Brillouin zone. After structural relaxation, the equilibrium lattice constant is found to be $a = 27.55$ a.u., that is 0.8% smaller than the experimental lattice constant. The binding energy as compared to the diamond phase is found to be 0.08 eV smaller, in good agreement with the results of Ref. [10]. In particular, the binding energy of this low density phase of Si is significantly larger than the one of the denser β-tin structure which can be shown to be ∼0.25 eV smaller than the one of the diamond phase. Further, using a Murnagham fit of the calculated energy points around the equilibrium volume, we obtain a bulk modulus of 87.7 GPa, which is 9.5% smaller than the value calculated for Si-2 within the same formalism (97.7 GPa). Our theoretical value for the bulk modulus of Si-34 is within the error bar of the measured value [7] $B_0 = 90 \pm 5$ GPa.

Using the LDA eigenstates as zeroth order wavefunctions (see above), we proceed with the GW calculation. As a byproduct of the calculation, we find a macroscopic dielectric constant of $\epsilon_M = 9.8$. This is ∼20% smaller than the 12.2 dielectric constant of Si-2 as calculated within the same formalism, indicating a reduced screening in the clathrate phase as compared to the diamond one. This reduction can be explained both by the larger gap and the smaller density of the clathrate.

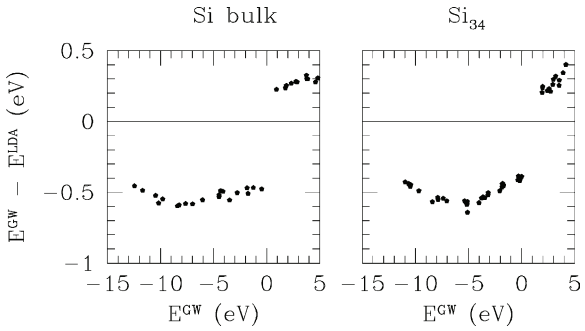

Fig. 2. Quasiparticle correction $E^{QP} - E^{LDA}$ as a function of the quasiparticle energies E^{QP} for Si-2 (left) and Si-34 (right). Energies are in eV.

We provide in Fig. 2 the quasiparticle correction to the DFT-LDA values both for the Si-2 and Si-34 type-II clathrate phase. The quasiparticle corrections are very similar. Using a fit of the data points displayed in Fig. 2, we can extrapolate the entire GW band structure from the one calculated within DFT. The result is provided in Fig. 3 together with the Si-46 quasiparticle band structure for which we have assumed a GW correction identical to the one obtained for Si-34. As a whole, the GW correction opens therefore the band gap by ∼0.6 eV, from 1.25 eV (LDA value) to

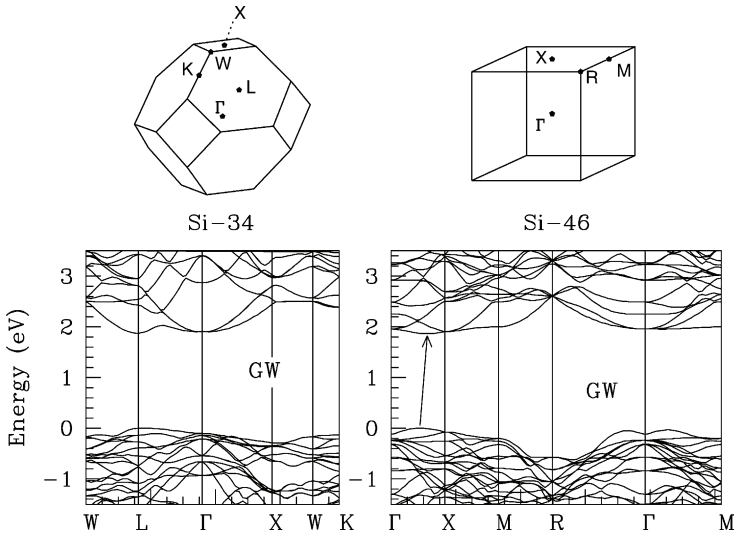

Fig. 3. Quasiparticle band structures of Si-34 and Si-46 along high-symmetry directions of the Brillouin zone. Energies are in eV. The zero has been set to the top of the valence bands.

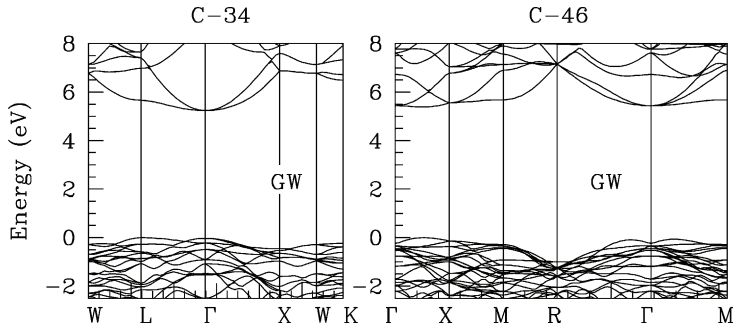

Fig. 4. Quasiparticle band structure of C-34 and C-46 along high-symmetry directions of the Brillouin zone. Energies are in eV. The zero has been set to the top of the valence bands.

∼1.85 eV in good agreement with available experimental results [29] and confirms the prediction based on DFT-LDA that the band gap of Si-34 is direct at L. While no detailed experimental mapping of the band-structure of Si-34 is available yet, the present results represent the most reliable account of the electronic properties of type-II Si clathrates.

2.3. The case of carbon clathrates

We now turn to the study of the hypothetical C-34 phase. Even though there is so far no evidence of the existence of such a phase, the report of the synthesis of crystals made out of connected C_{60} [30,31], C_{36} [32,33] or even C_{20} clusters [34] is a strong indication that carbon clathrates might be produced. Further, the synthesis of nanostructured thin-films with diamond-like properties by low energy deposition of free carbon clusters selected in mass [35], combined with the synthesis of free C_{20} clusters [36], is another evidence for the self-organization of small carbon clusters into a covalent-like network.

To account for the hardness of the carbon pseudopotential [24], we increase the energy cut-off for the planewave basis up to 40 Ry. After structural relaxation, we find the lattice constant of C-34 to be 18.06 a.u. The binding energy is only 0.10 eV smaller than the one of the C-2 phase [7,37] and the bulk modulus ∼14% smaller (398 GPa instead of 462 GPa). In particular, the hypothetical C-34 phase is less compressible than cubic BN which is 17% more compressible than diamond. We now perform quasiparticle calculations for the C-34 phase. We find a dielectric constant of 4.7, that is 16% smaller than the one of diamond (5.6 as calculated within the same formalism). The quasiparticle corrections for C-34 and C-2 are again very similar. The resulting quasiparticle band structure is provided in Fig. 4 together with the one of C-46. Within the GW formalism, we find a 5.15 eV band gap for C-34. The band gap is nearly direct at the zone center Γ but the top of the valence bands is found to be at L (even though degenerate with the one at Γ within 30 meV). For the C-46 type-I phase, the band gap is found to be nearly direct between Γ and X with a 5.25 GW value, the top of the valence bands and the bottom of the conduction bands being displaced by ∼0.05 ΓX.

Therefore, and contrarily to the Si case, the band gap of the hypothetical C-34 and C-46 phases would be actually smaller than the one of the diamond C-2 structure (5.6 eV within GW). This difference between Si- and C-based clathrates is yet to be understood. The accuracy of GW calculations for this kind of systems, as illustrated here in the case of Si-2, Si-34 and C-2, suggests that 5.15 eV should be within 0.1 eV the actual band gap of C-34 if ever synthesized.

3. Tayloring of the band gap by doping

The study presented in this section follows the synthesis by Reny et al. [4] of iodine doped I_8@Si-46 type-I clathrates. While n-type doped Na- or Ba-intercalated clathrates had been synthesized before, such a synthesis was the first case of doping by acceptors. Besides the case of iodine, other elements of the same line, from Sn to Xe, have been studied to assess the role of hybridization and ionicity in the

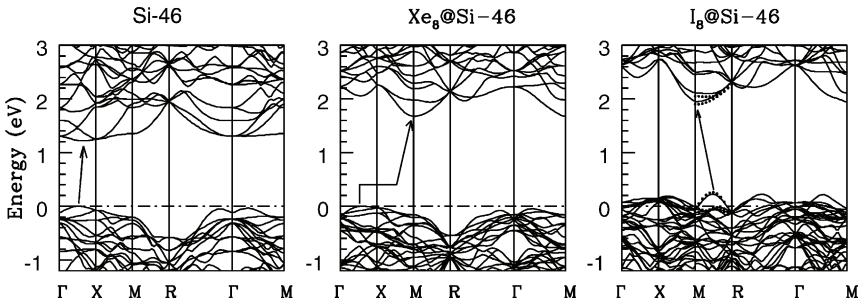

Fig. 5. DFT-LDA band structure of (left) Si-46, (center) Xe_8@Si-46 and (right) I_8@Si-46 along high symmetry directions of the Brillouin zone. Energies are in eV. The zero of energy has been set to the top of the valence bands for Si-46 and $XeXe_8$@Si-46 and to the Fermi level for IXe_8@Si-46. The dots indicate the all-electron calculation values (see Ref. [38]). The arrows indicate the nature of the gap.

evolution of the electronic properties under doping. More details can be found in a previous work by Connétable et al. [5].

We provide in Fig. 5 the LDA band structure of I_8@Si-46 along high-symmetry directions of the Brillouin zone. Due to the electronegativity of iodine, the Fermi level E_F is located 0.26 eV below the energy gap. I_8@Si-46 is therefore a p-type doped semiconductor. The comparison of the I_8@Si-46 and Si-46 band structures clearly shows that the ''rigid-band-model'', consisting of a shift under doping of the Fermi level without modification of the host network band structure, is not appropriate for the present system, in great contrast with the case of Ba_xNa_{8-x}@Si-46 compounds. In particular, we find that *the band gap is increased from 1.2 to 1.75 eV under doping* (DFT value).

The case of Xe_8@Si-46, which displays a 1.65 eV band gap, reveals that ionic effects are not at the origin of such a band gap opening. From the comparison of the band structure of Si-46 and Xe_8@Si-46 (Fig. 5), we find that the top of the valence bands is only slightly modified upon introduction of the Xe atoms, while the bottom of the conduction bands changes dramatically as in IXe_8@Si-46. This indicates that the coupling between the Xe (or I) orbitals take place mainly with the bottom of the conduction bands, thus opening the band gap by repulsion. The analysis of the symmetry character of the Si-46 states at Γ (O_h group) shows that the top of the valence and bottom of the conduction bands belong respectively to the A_{1u} and T_{1u} representations. The set of representations into which the Xe or I orbitals split in the O_h crystal field includes T_{1u} but not A_{1u} so that indeed only the bottom of the conduction bands can couple to the intercalated atom orbitals.

We have analyzed further the evolution under intercalation of the Kohn–Sham spectrum of the $Si_{20}H_{20}$, $Si_{24}H_{24}$ and $Si_{28}H_{28}$ cages. Hydrogen passivation is used to mimic the sp^3 character of the Si atoms in the bulk clathrate phase. Again, at the DFT-LDA level, we find the band gap of the Si_nH_n clusters to increase from 0.5 eV to 0.9 eV under Xe doping (the smallest the cage, the larger the correction). Only low-lying unoccupied levels are affected by intercalation. This can again be understood on the basis of group symmetry analysis of the cage states and Xe-(s, p) levels in the I_h ($n = 20$), D_{6d} ($n = 24$) and T_d ($n = 28$) point group of the Si_nH_n cages. The densities of state of pure and doped $Si_{20}H_{20}$ clusters are given in Fig. 6.

Performing further a GW calculation for the insulating Xe_8@Si-46 phase, we find a ∼0.7 eV correction to the DFT-LDA band gap, which is similar to what was found for empty clathrates or the Si-2 diamond phase. From the present set of calculations, it stems that Xe_8@Si-46 displays a quasiparticle band gap of ∼2.25 eV and is thus a silicon based ''green light'' semiconductor system. Such a result suggests that *doped-clathrates may be potentially important in the making of silicon-based opto-electronic devices*.

In the case of type-I clathrates, we find the band gap to be indirect (see Fig. 7). However, if we now concentrate on the type-II Xe doped system, we find the band gap of Xe_6@Si-34 to be direct with an LDA value of 1.95 eV, that is ∼2.5 eV within the GW approximation. Analysis of the symmetries shows however that the HOMO and LUMO states (at the

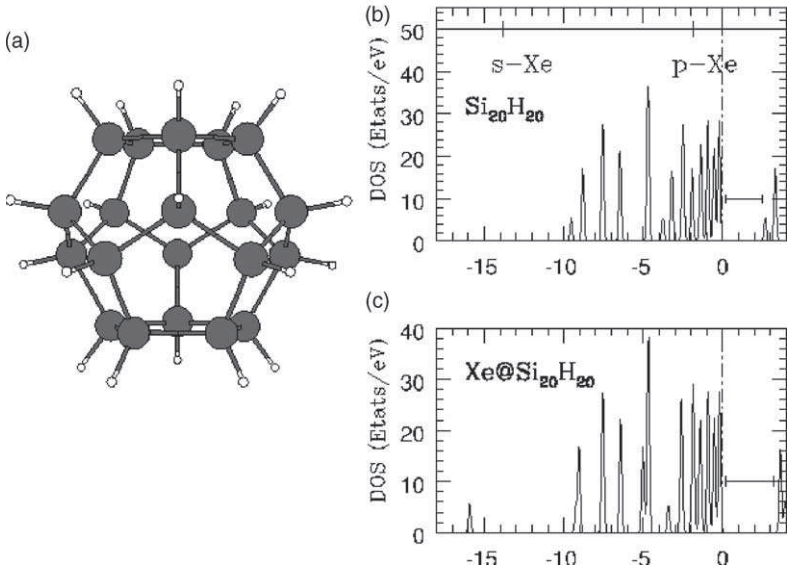

Fig. 6. (a) Symbolic representation of $Si_{20}H_{20}$. Parts (b) and (c) show eDOS for the empty and Xe-intercalated cages. The zero has been set to the top of the valence bands and the gaps have been indicated by horizontal lines. Atomic 5s,p levels of the isolated Xe atoms are given above the eDOS.

L point) are respectively of E_g and A_{1g} character and no optical transition is allowed. Even though transitions become allowed away from the L point along the LΓ direction, it is clear that photoluminescence will be poor in such systems. The search of clathrate-like structures presenting different symmetries may lead however to materials where the optical transitions will be allowed.

4. Superconductivity in Ba-doped clathrates

A striking consequence of the possibility of doping insulating silicon clathrates is the occurrence of superconductivity in Ba_8@Si-46 [6]. In such a compound, it has been shown that a strong hybridization of Ba 5d and Si 3p states occurs in the conduction bands, yielding a large eDOS at the Fermi level (E_F). To study the origin of superconductivity and try to assess if the superconducting transition is associated with Ba or may occur with other type of doping, we have studied ab initio the electron–phonon coupling strength in such materials. Our approach is based on the use of the perturbative density functional theory (DFPT) implemented in the PWSCF package [39]. The ab initio calculation of the perturbation $(\delta V/\delta \boldsymbol{R})$ of the total ionic plus self-consistent electronic potential associated with the phonon modes allows to obtain

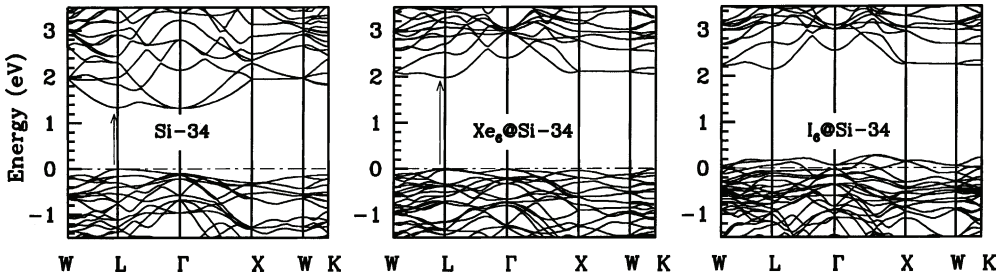

Fig. 7. DFT-LDA band structure of (left) Si-36, (center) Xe_6@Si-34 and (right) I_6@Si-34 along high symmetry directions in the Brillouin zone. The arrows indicate the nature of the gap.

Table 1
λ, $N(E_F)$ (in states/eV cell) and V_{ep} (in meV) for X_8@Si-46 doped by X = Ba, I and Na

X element	λ	$N(E_F)$	V_{ep}
Ba	1.05	43	24
I	0.90	44.4	20
Na	0.40	15.3	26

the electron–phonon matrix elements $\langle\psi^0_{nk}|\hat{\varepsilon}_{qv}\cdot(\delta V/\delta \boldsymbol{R})|\psi^0_{nk+q}\rangle$, which can be used to evaluate the electron–phonon coupling constant λ or the average electron–phonon interaction potential V_{ep}. More details about the formalism can be found in Ref. [40].[5] The knowledge of $\boldsymbol{\lambda}$ allows to compute T_c following McMillan [41]:

$$T_c = \frac{\hbar\omega_{log}}{1.2k_B}\exp\left[\frac{-1.04(1+\lambda)}{\lambda-\mu^*(1+0.62\lambda)}\right]$$

where μ^* is the effective electron–electron repulsive interaction and ω_{log} an effective phonon energy.

Our preliminary results [42] show that the superconductivity of Ba_8@Si-46 is an intrinsic property of the silicon network. The role of barium is merely to provide charge to the clathrate network. We indeed doped the network by other elements than barium, such as iodine (p-type doping), and found that the coupling constant λ is similar (see Table 1). In the case of Na_8@Si-46 where no superconductivity has been observed down to 2 K, the average electron–phonon interaction potential V_{ep} is actually similar to the one obtained with Ba and I, indicating an efficient electron–phonon coupling, but the low density of states $N(E_F)$ leads to a small value of λ which can explain that T_c is small. Using a rigid-band model, we artificially doped further the silicon diamond phase. Again, for equivalent density of states at the Fermi level, the same coupling constant λ is found, yielding an equivalent T_c if we assume that the effective electron–electron repulsion μ^* is constant from one phase to another.

The superconductivity of sp^3 silicon has never been addressed as it is well known that doping the dense diamond network is difficult. In the case of diamond, the impossibility of injecting enough charge to have a reasonable density of states at the Fermi level hindered any superconducting transition. In the case of clathrates, intercalation at the center of the cages allows significant doping of the network and allows to observe the onset of superconductivity in such materials. The case of doped carbon clathrates has been further studied indicating a new route towards the synthesis of large T_c compounds. More details will be given in a forthcoming publication [42].

[5] We follow the notations of [40].

5. Conclusion

In conclusion, we have studied the electronic and superconducting properties of silicon and carbon clathrates. While empty silicon clathrates display interesting properties with a band gap ~0.6 eV larger than in the diamond phase, the most interesting properties are revealed by doping such phases. On the basis of accurate GW calculations, it is shown that doping of clathrates can lead to materials with a direct band gap in the visible. Unfortunately, the transitions are found to be dipole-forbidden for the structures studied. Further, the possibility of significantly doping such sp^3 systems by intercalation allows to study the superconducting properties of the sp^3 network. We find that the ~8 K transition temperature measured for Ba_8@Si-46 is an intrinsic properties of the silicon network and that other type of doping will lead to similar superconducting properties, provided that the density of states at the Fermi level is large enough. Such a result leads to interesting properties in the case of the clathrate carbon phase.

Acknowledgements

The authors are indebted to V. Timoshevskii, A. san Miguel, P. Mélinon, C. Cros, M. Pouchard and S. Yamanaka for numerous discussions concerning the physics of clathrates and for providing the experimental results which motivated this work. Calculations have been performed at the French CNRS national computer center at IDRIS (Orsay).

References

[1] J. Kasper, P. Hagenmuller, M. Pouchard, C. Cros, Science 150 (1965) 1713.

[2] S. Yamanaka, E. Enishi, H. Fukuoka, M. Yasukawa, Inorg. Chem. 39 (2000) 56.
[3] F. Brunet, et al., Phys. Rev. B 61 (2000) 16550.
[4] E. Reny, S. Yamanaka, C. Cros, M. Pouchard, Chem. Commun. 24 (2000) 2505.
[5] D. Connétable, V. Timoshevskii, E. Artacho, X. Blase, Phys. Rev. Lett. 87 (2001) 206405.
[6] H. Kawaji, H. Horie, S. Yamanaka, M. Ishikawa, Phys. Rev. Lett. 74 (1995) 1427;
J.D. Bryan, V.I. Srdanov, G.D. Stucky, D. Schmidt, Phys. Rev. B 60 (1999) 3064;
S. Yamanaka, E. Enishi, H. Fukuoka, M. Yasukawa, Inorg. Chem. 39 (2000) 56–58.
[7] A. San-Miguel, P. Kéghélian, X. Blase, P. Mélinon, A. Perez, J.P. Itié, A. Polian, E. Reny, C. Cros, M. Pouchard, Phys. Rev. Lett. 83 (1999) 5290.
[8] J.L. Cohn, G.S. Nolas, V. Fessatidis, T.H. Metcalf, G.A. Slack, Phys. Rev. Lett. 82 (1999) 779.
[9] J.S. Tse, K. Uehara, R. Rousseau, A. Ker, C.I. Ratcliffe, M.A. White, G. MacKay, Phys. Rev. Lett. 85 (2000) 114.
[10] G.B. Adams, M. O'Keeffe, A.A. Demkov, O.F. Sankey, Y.-M. Huang, Phys. Rev. B 49 (1994) 8048.
[11] P. Hohenberg, W. Kohn, Phys. Rev. B 136 (1964) 864;
W. Kohn, Rev. Mod. Phys. 71 (1999) 1255.
[12] S. Saito, A. Oshiyama, Phys. Rev. 51 (1995) 2628.
[13] V.I. Smelyanski, J.S. Tse, Chem. Phys. Lett. 264 (1997) 459.
[14] P. Mélinon, P. Kéghélian, X. Blase, J.L. Brusc, A. Perez, E. Reny, C. Cros, M. Pouchard, Phys. Rev. B 58 (1998) 12590.
[15] K. Moriguchi, S. Munetoh, A. Shintani, Phys. Rev. B 62 (2000) 7138.
[16] W. Kohn, L.J. Sham, Phys. Rev. A 140 (1965) 1133.
[17] E. Galvani, G. Onida, S. Serra, G. Benedek, Phys. Rev. Lett. 77 (1996) 3573–3576.
[18] L.J. Sham, M. Schlüter, Phys. Rev. Lett. 51 (1983) 1888.
[19] X. Blase, X. Zhu, S.G. Louie, Phys. Rev. B 49 (1994) 4973;
M. Rohlfing, P. Krüger, J. Pollmann, Phys. Rev. B 52 (1995) 1905;
O. Pulci, G. Onida, R. Del Sole, L. Reining, Phys. Rev. Lett. 81 (1998) 5374.
[20] L. Hedin, Phys. Rev. A139 (1965) 796;
L. Hedin, S. Lundqvist, Solid State Phys. 23 (1969) 1.
[21] M.S. Hybertsen, S.G. Louie, Phys. Rev. Lett. 55 (1985) 1418;
M.S. Hybertsen, S.G. Louie, Phys. Rev. B 32 (1985) 7005;
M.S. Hybertsen, S.G. Louie, Phys. Rev. B 34 (1986) 5390;
R.W. Godby, M. Schlüter, L.J. Sham, Phys. Rev. Lett. 56 (1986) 2415;
R.W. Godby, M. Schlüter, L.J. Sham, Phys. Rev. B 37 (1988) 10159.
[22] M.S. Hybersten, S.G. Louie, Phys. Rev. B 35 (1987) 5585, and references therein.
[23] S.L. Adler, Phys. Rev. 126 (1962) 413;
N. Wiser, Phys. Rev. 129 (1963) 62.
[24] N. Troullier, J.L. Martins, Phys. Rev. B 43 (1991) 1993.
[25] K. Kleinman, D.M. Bylander, Phys. Rev. Lett. 48 (1982) 1425.
[26] J.P. Perdew, A. Zunger, Phys. Rev. B 23 (1981) 5048.
[27] D.M. Ceperley, B.J. Alder, Phys. Rev. Lett. 45 (1980) 566.
[28] H.J. Monkhorst, J.D. Pack, Phys. Rev. B 13 (1976) 5188.
[29] J. Gryco, P.F. McMillan, R.F. Marzke, G.K. Ramachandran, et al., Phys. Rev. B 62 (2000) R7707.
[30] L. Marquez, M. Mezouar, J.L. Hodeau, M. Nunez-Rigueiro, Science 283 (1999) 1720.
[31] S. Okada, S. Saito, A. Oshiyama, Phys. Rev. Lett. 83 (1999) 1986.
[32] C. Piskoti, J. Yarger, A. Zettl, Nature 393 (1998) 771.
[33] P.G. Collins, J.C. Grossman, M. Csuperioroté, M. Ishigami, C. Piskoti, S.G. Louie, M.L. Cohen, A. Zettl, Phys. Rev. Lett. 82 (1999) 165.
[34] Z.X. Wang, X.Z. Ke, Z.Y. Zhu, F.Y. Zhu, M. Ruan, H. Chen, R. Huang, L. Zheng, Phys. Lett. A 280 (2001) 351.
[35] V. Paillard, P. Mélinon, V. Dupuis, J.P. Perez, A. Perez, B. Champagnon, Phys. Rev. Lett. 71 (1993) 4170.
[36] H. Prinzbach, A. Weller, P. Landenberger, F. Wahl, J. Wörth, L.T. Scott, M. Gelmont, D. Olevano, B.V. Issendorff, Nature (London) 407 (2000) 60.
[37] M. Bernasconi, S. Gaito, G. Benedek, Phys. Rev. B 61 (2000) 12689.
[38] An all electron-calculation was performed using the FLAPW WIEN97 package, see: P. Blaha, K. Schwarz, J. Luitz, Technical University of Vienna, Austria, ISBN 3-9501031-0-4, Scalar-relativistic effects were included in the muffin-tin spheres. We have studied the MR direction for the I_8@Si-46 compound. Aligning the Fermi levels, we find that around the gap the all-electron and pseudopotential calculations agree within better than 0.1 eV (see Fig. 5).
[39] S. Baroni, S. de Gironcoli, A. Dal Coso, P. Giannozzi, Rev. Mod. Phys. 73 (2) (2001) 515;
S. Baroni, A. Dal Corso, S. de Gironcoli, P. Giannozzi, http://www.pwscf.org.
[40] M.M. Dacarogna, M.L. Cohen, Phys. Rev. Lett. 55 (1985) 837.
[41] W.L. McMillan, Phys. Rev. 167 (1968) 331.
[42] D. Connétable, et al., Phys. Rev. Lett. (in press).